The effect of the atomic relaxation around defects on the electronic structure and optical properties of β-SiC

1999 J. Phys.: Condens. Matter 11 2265

(http://iopscience.iop.org/0953-8984/11/10/013)

J. Phys.: Condens. Matter **11** (1999) 2265–2278. Printed in the UK PII: S0953-8984(99)97680-4

The effect of the atomic relaxation around defects on the electronic structure and optical properties of β-SiC

G Cubiotti†‡, Yu Kucherenko§, A Yaresko§, A Perlov§ and V Antonov§

† Dipartimento di Fisica, Sezione di Fisica Teorica, Università di Messina, PO Box 50, 98166 Sant'Agata di Messina, Messina, Italy
‡ Istituto Nazionale di Fisica della Materia, Unità di Messina, Messina, Italy
§ Institute of Metal Physics, National Academy of Sciences of Ukraine, Vernadsky Street 36, 252142 Kiev, Ukraine

Received 17 September 1998, in final form 8 December 1998

Abstract. The electronic structure and the optical properties associated with antisite defects in cubic SiC have been computed by means of the LMTO (linear muffin-tin orbital) method and the supercell approach. The orbital-dependent LDA + U potential (LDA $\equiv$ local density approximation) used in the present work gives rise to an improved description both of the electronic structure near the energy gap and of the optical functions. Attention has been mainly focused on the effects caused by the local lattice relaxation around the defects. For compositions that deviate from the stoichiometric SiC towards higher content of carbon atoms, the small reduction of the energy gap which is observed experimentally can be explained only if the lattice relaxation is taken into account. The local electronic structure of antisite defects is characterized by s- and p-like resonance states in the valence band. Strong resonances occur also in the conduction band (especially for C_{Si}). The Si_C (C_{Si}) antisite has more (fewer) valence electrons localized in the atomic sphere than the *official* Si (C) atom, but this difference is considerably reduced by the lattice relaxation. The results of the calculations show how the presence of point defects modifies the shape of the optical functions of the perfect SiC crystal and how the lattice relaxation has a strong effect on the fine structure of the optical functions. Different kinds of defect lead to different shapes of the optical functions.

1. Introduction

In the past few years a great deal of theoretical investigation has been devoted to the electronic structure of the different phases and polytypes of SiC, because of its interesting properties and the possibilities of its use in electronic devices [1–8]. However, in spite of recent advances in crystal growth capability, there are small deviations from stoichiometry, and even small deviations can give rise to significant concentrations of native defects, such as vacancies, antisites and self-interstitial defects. These defects can, in turn, affect the behaviour and the efficiency of the material in electronics applications.

The electronic properties of cubic (zinc-blende) β-SiC containing different kinds of native defect have recently been studied theoretically by means of different methods of calculation [9–11]. In all of these calculations no lattice relaxation around the defects has been allowed for and neutral defects have been considered.

In this work we present the results of a theoretical study of the electronic structure and of the optical properties of the β-SiC polytype containing the Si_C antisite (where a Si atom has been substituted for a C atom), the C_{Si} antisite (where a C atom has been substituted for a Si

0953-8984/99/102265+14$19.50

atom) and a pair of point defects where the antisites of different kinds are first neighbours to each other. The results of the theoretical estimation [12] show that antisite defects (especially C_{Si}) have lower formation energies than other kinds of point defect in SiC. On the other hand, the presence of antisite defects gives rise to a significant lattice distortion: relative changes in the interatomic distances around the defect can be as large as 8–12% [12]. Thus, we have paid special attention to the effects of the lattice relaxation on the energy distribution of the valence electron states, on the electronic charge on the atoms, on the character of chemical bonding and, consequently, on the optical properties of the crystal.

As in [8], the calculations have been performed using the LMTO method. In order to describe the crystal structure containing defects we have used a supercell approach. Within this approach it has been possible to take into account the lattice relaxation around defects in the most simple and natural way.

The paper is organized as follows. In section 2 we describe the structure of the supercell and the computational details. In section 3 the results of the electronic structure calculations are discussed. The calculated optical functions for the non-perfect β-SiC crystal are presented in section 4. Conclusions are drawn in section 5.

2. The structure model and computational details

2.1. The choice of supercell

The atomic structure of β-SiC can be understood if one considers a stacking sequence of hexagonal bilayers, consisting of pairs of Si and C layers with tetrahedral bonds between atoms. Successive bilayers are displaced sideways, so atoms in each bilayer are characterized by one of the possible positions A $(0, 0, z_1)$, B $(1/3, 2/3, z_2)$ and C $(2/3, 1/3, z_3)$. The vertical sequence of bilayers in the cubic β-SiC polytype is ABCABC . . .. The supercell that we have considered in our model contains eighteen atoms (nine Si atoms and nine C atoms in the case of the perfect crystal). It contains three bilayers with six atoms each (three atoms in each layer), characteristic of the cubic structure. If a point defect (or a pair of the neighbouring point defects) is created in this supercell, other defect sites can be found as far as fourth neighbours. It has been shown in our preliminary consideration [13] that the perturbation of the electron density caused by defects is already weak for the second neighbour. Thus, we assume that the interaction of point defects located in different supercells can be considered negligible.

2.2. The method of calculations

As in [8], the energy band structure has been calculated by means of the self-consistent LMTO method in the atomic-sphere approximation and including combined corrections (ASA + CC). A detailed description of the method can be found in [14] and [15]. In order to obtain a close-packed structure, empty spheres have been introduced in the interstitial regions, with the result that the total number of spheres in the supercell was 36. The calculations have been performed within the scalar-relativistic formalism for the valence states, whereas full relativistic solutions have been used for the core levels. The exchange and correlation effects have been taken into account by using the local density approximation (LDA) and the von Barth–Hedin parametrization for the exchange–correlation potential [16]. The angular momentum expansion of the basis functions has been performed up to $l = 2$ for all of the spheres. The electron density of states (DOS) has been computed by using the Brillouin zone integration method described in [17]. Calculations have been performed for 238 irreducible $\boldsymbol{k}$-points of the Blöchl mesh (4109 tetrahedra have been used for the Brillouin zone integration).

The calculated results were considered self-consistent if the largest charge-density variation was less than 10^{-5} atomic units with respect to the preceding iteration. As discussed in [8], taking into account the combined corrections produces results which show a very weak dependence on the choice of the atomic radii. We have used for the atomic sphere radii the following values: 2.2357 au for Si atoms, 1.9207 au for C atoms, 1.8054 au for empty spheres surrounded by 'large' Si atoms and 2.1016 au for empty spheres surrounded by 'small' C atoms. According to the atomic sphere approximation, the sum of the volumes of all of the spheres in the cell should be equal to the volume of the supercell, and therefore in the case of the presence of antisite defects this sum has been corrected by varying the radii of empty spheres surrounding the defect.

The imaginary part $\varepsilon_2(\omega)$ of the dielectric function has been calculated within the one-electron self-consistent-field approach [18] using the momentum transition-matrix elements. The interband contribution to the real part of the dielectric function $\varepsilon_1(\omega)$ has been obtained by Kramers–Kronig analysis. The results presented have been averaged over the light polarizations and 200 energy bands have been used in the calculations. Use of a limited number of bands leads to underestimated values of ε_2 for $\hbar\omega > 46$ eV. Thus we can estimate that the Kramers–Kronig analysis is valid at least up to 25 eV. The calculated optical functions have been convoluted with a Gaussian of 0.05 eV FWHM to account for the finite experimental resolution.

2.3. The LDA + U approach

Because of the well-known underestimation of the band gap by calculation methods using LDA, a comparison of calculated results with experimental data requires the consideration of the self-energy effects on single-particle excitations. To solve this problem one should take into account quasiparticle corrections which have, in general, non-local character [19]. In order to retain the local character of the potential in the theoretical model used and to avoid more complicated calculations, some authors included these corrections in the simplest manner, namely as a constant energy shift of the calculated spectra [3,8]. However, in the present work we have chosen to overcome the deficiency of the LDA by means of the so-called LDA + U method [20]. In this approach the non-local and energy-dependent self-energy is approximated by a frequency-independent but non-local screened Coulomb potential. With this orbital-dependent LDA + U potential the orbital polarization becomes possible and the LDA failure in describing the band gap can be removed. The LDA + U method was initially developed for the theoretical description of the electronic structure in strongly correlated systems [21, 22] and seems to be applied to the semiconductors for the first time in the present work. It has been shown in [20] that the LDA + U theory may be regarded as an approximation to the GW-theory [23, 24] which is widely used in different modifications in order to take into account the quasiparticle effects in semiconductors [6, 25]. In principle, the LDA + U method could be applied as an *ab initio* approach where the parameters U_l are estimated from the calculated energies of the on-site excitations (using the Slater transition-state concept). However, in order to reduce the computational effort, we have used a simplified approach. We have introduced the additional potentials U_l only for the valence p states of carbon and silicon and we have estimated the values of the potentials U_p(C) and U_p(Si) by fitting the calculated values for the fundamental energy gap to the experimental ones [26] for the diamond and for the silicon crystals, respectively. We have obtained $U_p(\mathrm{C}) = 3.78$ eV and $U_p(\mathrm{Si}) = 2.18$ eV. Then we performed the LDA + U calculations of the electronic structure in the perfect β-SiC crystal using these values for C and Si atoms. The calculations gave a value of the indirect energy gap equal to 2.395 eV, in excellent agreement with experiment (2.39 eV [26] or 2.417 eV [27]).

It should be noted that this gap value has been obtained without any additional fitting of the U-parameters. The agreement achieved with the experimental data could be considered as evidence that in SiC crystals the electron states are localized enough to be accurately described within the LDA + U approach. The LDA + U approach has also improved the calculated results for optical properties. It can be seen in figure 1 that the low-energy shifts of most of the features in the optical functions, which take place in the LDA, are eliminated in the LDA + U method. Thus, in the following calculations for defect-containing SiC crystals the LDA + U method with two parameters U_p(C) and U_p(Si) has been used.

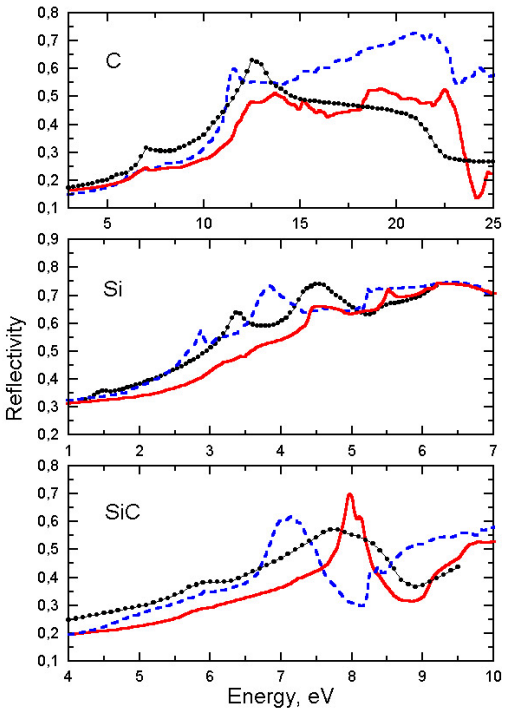

Figure 1. The reflectivity functions for diamond, silicon and β-SiC calculated using the LDA (dashed curves) and LDA + U (solid curves) approaches. The experimental results (solid circles) are from [28–30].

3. Local electronic structure around defects

3.1. Single antisite defects

The size differences between the carbon and silicon atoms give rise to the lattice relaxation around antisite defects. The nearest-neighbour atoms are shifted inwards (for the C_{Si} antisite) or outwards (for the Si_C antisite), and these atomic shifts maintain a T_d symmetry around the defect. According to the published results of pseudopotential [12, 31] and tight-binding [10] calculations, the nearest-neighbour atoms around the Si_C antisite relax by 12–14% of the interatomic distance whereas in the case of the C_{Si} antisite the calculated values for the changes in the nearest-neighbour distances are quite different: 8% [12], 11% [31], almost 15% [10]. Our estimation of the formation energies for the different kinds of point defect in β-SiC provides results which agree fairly well with values given in [12]. However, in the LMTO method

used in the present work the small changes in the calculated total-energy value could be due to changes in the overlapping of the atomic spheres or in the atomic sphere radii. These effects interfere with the accurate estimation of atomic shifts caused by relaxation. Therefore we discuss the effects which are already essential for a minimal degree of the atomic relaxation: the 8% inwards shift around the C_{Si} antisite and the 12% outwards shift around the Si_C antisite.

Let us consider the effect of point defects on the value of the fundamental optical gap. In the case of the Si_C antisite, Si–C bonds are replaced by weaker Si–Si bonds. The electron states related to these Si–Si bonds lie just at the band edges (at the top of the valence band and at the bottom of the conduction band) and are responsible for the changes in the energy gap. Thus, we could expect a decreasing of the gap mainly due to an increasing of the value of the valence band top [32]. For the C_{Si} antisite a similar qualitative consideration cannot lead to any clear result because of the position of the electron states related to the strong C–C bonds. In fact, these electron states lie within the bands and cannot determine the value of the energy gap directly. They could play some role but only by means of interaction with the Si–C bonds. Most theoretical models predict further increasing of the energy gap in the Si–C compounds if the composition deviates from stoichiometric SiC towards a higher content of carbon atoms (see [32]). This is however in contradiction with experimental results [33–35] where the energy gap value tends to show a maximum for compositions close to that of the stoichiometric SiC crystal.

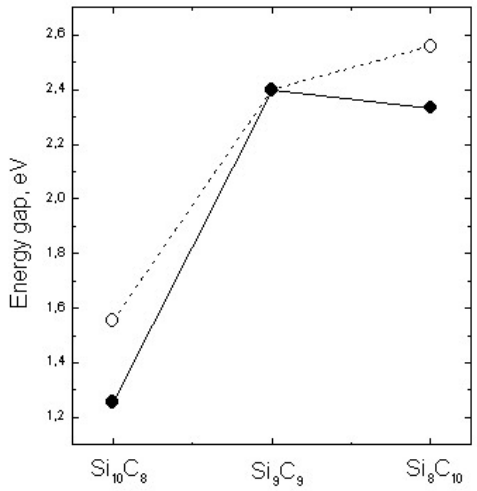

Figure 2. The calculated values of the energy gap for the perfect SiC crystal and for crystals containing antisite defects (the atomic composition of supercell is indicated) without (open circles) and with lattice relaxation (solid circles).

Our calculated results are presented in figure 2. One Si_C antisite per supercell causes considerable decreasing of the energy gap. The lattice relaxation tends to lengthen Si–Si bonds, and this leads to a further reduction of the energy distance between the pertinent bonding and antibonding electron states. In the case of the non-relaxed lattice around the C_{Si} antisite, our calculations indicate a small increasing of the energy gap. Due to the lattice relaxation, the C–C bonds become shorter but the inwards shift of the carbon atoms surrounding C_{Si} tends to stretch the bonds to the next Si atoms. This should reduce the energy gap, because in the case of the C_{Si} antisite the band edges are determined by the electron states related to the Si–C bonds. Thus, the energy gap value is smaller than that for the perfect stoichiometric SiC crystal. It

should be noted that further inwards shift of carbon atoms surrounding antisite defects (with the tendency to create a diamond-like tetrahedral carbon cluster) leads to a further reduction of the energy gap. For example, in the case of a 14% inwards relaxation, our calculations give an energy gap of 1.97 eV. If we assume that antisite defects are the main kind of point defect for compositions which deviate from that of the stoichiometric SiC compound [12], the calculated dependence of the energy gap on the crystal composition agrees well with the results of the experimental measurements.

In [32] the decreasing of the energy gap for increasing carbon content is explained as being due to the advent of the C sp^2 bonding and also the effect of π-bonded electron states. This possibility could be realized in the case of the graphite-like clustering of carbon atoms by the decreasing of the local symmetry around the C_{Si} antisite from T_d to C_{3v}. In the SiC crystal the vacancy–antisite complex is suitable for being organized in a graphite-like clustering, and this situation will be discussed in our forthcoming work. Here we have shown however that the energy gap decreases even in the case of the diamond-like tetrahedral clusters of C atoms, if the lattice relaxation around C_{Si} antisites is taken into account.

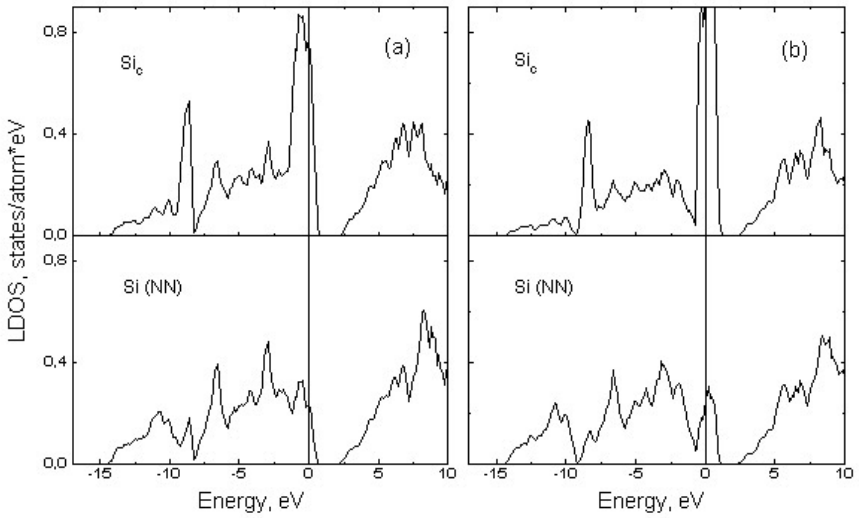

Figure 3. The calculated local densities of electron states for Si_C sites and for nearest-neighbour Si atoms without (a) and with the lattice relaxation taken into account (b).

In figures 3 and 4 the local DOS at Si and C sites are displayed. The vertical line in each figure indicates the valence band maximum for the perfect crystal. It can be seen that, as in earlier calculations [9–12], no defect-induced states exist in the gap. The Si_C antisite presents a p-like resonance state just below the valence band top and an s-like resonance state at -9.04 eV which is shifted to the energy -8.46 eV after lattice relaxation. These results agree with those in [11] where the calculations, performed by means of a tight-binding LMTO Green-function method, show a p-like resonance below the valence band maximum and an s-like resonance at -7.0 eV for the case of the Si_C antisite. Some differences in the calculated energy positions of resonances could be explained by the effect of the additional orbital-dependent potential introduced in our work within the LDA + U approach. In the conduction band the weak defect-induced resonance having p character could be found at +6.67 eV. Due to the lattice relaxation, it is shifted towards the high-energy side, and the energy distribution of unoccupied electron

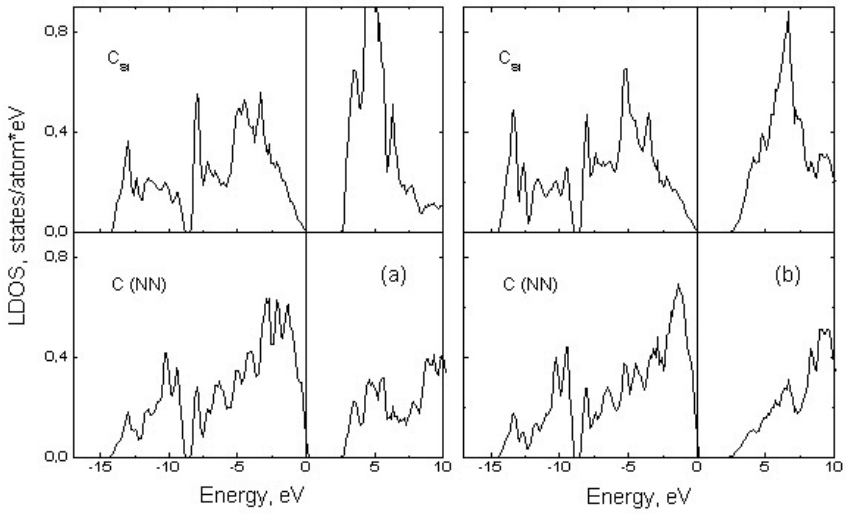

Figure 4. The calculated local densities of electron states for C_{Si} sites and for nearest-neighbour C atoms without (a) and with the lattice relaxation taken into account (b).

states at the Si_C antisite becomes very close to the local DOS at the sites of the non-perturbed Si atoms. The p-like resonance is the most prominent feature in the local DOS of the Si_C antisite. These Si p states are responsible for displacement of the valence band top towards higher energies and for reduction of the energy gap. They could also give rise to the split states observed at 0.2–0.4 eV above the maximum of the valence band (so-called H centres) which are discussed in [31] and interpreted as ionization states of Si_C antisites.

In the case of the C_{Si} antisite we have found a p-like resonant state at -4.62 eV and an s-like resonant state at the bottom of the valence band. Both resonances have then been enhanced by the lattice relaxation. We would not interpret the peak at the energy of -7.95 eV (in [11] in this case an s-like resonance at -7.0 eV is reported) as a defect-induced state, because this sharp peak is a characteristic feature in the DOS of the valence s electrons even in the case of non-perturbed carbon atoms in the SiC crystal. The most prominent feature in the local electronic structure of the C_{Si} antisite is the high resonance in the conduction band at +4.62 eV. These states substantially disturb the behaviour of the local DOS at the nearest-neighbour C-atom sites. The lattice relaxation shifts these unoccupied C p states to +6.67 eV, and a small shift of the occupied resonance states in the valence band towards lower energies can be also found. Thus, in the relaxed lattice the energy distance between bonding and antibonding states related to the C–C bonds increases. It should also be noted that, after the lattice relaxation is taken into account, the shape of the local DOS in the conduction band at the nearest-neighbour C-atom sites becomes close to that at the sites of the non-perturbed carbon atoms.

The valence electron charge localized in the atomic spheres is shown in figure 5 for the antisite atoms and for their neighbours. The partial composition of the valence electron charge for different cases is given in table 1. In the perfect SiC crystal the Si atomic sphere contains fewer valence electrons than the C atomic sphere in spite of the large radius of the Si atomic sphere. Therefore the Si–C bond could be considered as polarized, with a shifting of the electron charge towards the carbon atom. It can be seen that at the Si_C antisite there is a larger amount of electron charge with respect to the *official* Si site and that also there is extra charge on the nearest neighbours of the defect. This could be thought of as due to the fact that the

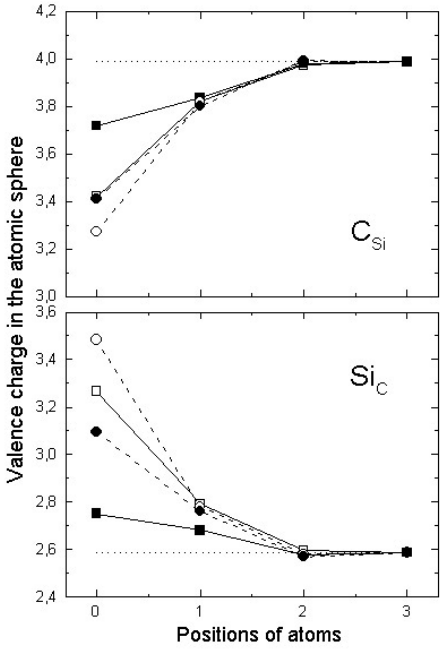

Figure 5. The valence electronic charge in C and Si atomic spheres around single (circles) and paired (squares) antisite defects: (0) the defect atom, (1) the nearest-neighbour atom, (2) the third neighbour, (3) the atom in the perfect crystal. The calculated results for the non-relaxed lattice are denoted with open symbols, those for relaxed lattice with solid symbols.

Table 1. Valence electron charges in the ASA spheres.

Valence charge	Perfect crystal	Single antisite		Antisite pair	
		Non-relaxed	Relaxed	Non-relaxed	Relaxed
C (total)	3.987	3.272	3.413	3.418	3.717
s	1.161	1.114	1.076	1.127	1.075
p	2.785	2.084	2.212	2.217	2.492
d	0.041	0.074	0.125	0.074	0.150
Si (total)	2.588	3.483	3.095	3.266	2.751
s	0.860	1.059	1.011	1.036	0.930
p	1.394	2.230	1.945	2.005	1.620
d	0.334	0.194	0.139	0.225	0.201

silicon atoms hold an extra electron charge, which is usually shifted to neighbouring carbon atoms in the case of the *official* Si site. The behaviour of the C_{Si} antisite is the reverse of that in the Si case. C_{Si} loses electronic charge in comparison with the *official* C sites (or, in other words, it could not withdraw electronic charge from neighbouring atoms due to the absence of Si atoms around C_{Si}). The changes in the charge of the nearest neighbours amount to about 0.2 electrons. Next, atoms of the same kind (third neighbours) show only negligible deviation of the valence electron charge from the *official* value. The Si_C antisite gains almost 0.9 e whereas the C_{Si} antisite loses about 0.7 e. When reduced by the lattice relaxation, these values amount to 0.51 e and 0.57 e for Si_C and C_{Si}, respectively. It should be noted that the relaxation has no

significant effect on the valence charge of the nearest-neighbour atoms, in spite of the actual shift of these atoms in the relaxation process.

The changes in the valence electron charge at the antisite defects are caused essentially by p electrons and, to some extent, also by s electrons. The valence d states show an opposite behaviour: an increasing number of d electrons for the C_{Si} antisite and a decreasing one for the Si_C antisite. This behaviour could reflect an increased localization of the electron states along C–C bonds and a decreased one along Si–Si bonds, as compared to the Si–C bonds in the perfect SiC crystal. The lattice relaxation leads to an increasing number of p and d electrons if the interatomic distance is reduced. If the surrounding atoms are shifted outwards from the defect, the number of p and d electrons in the antisite atomic sphere decreases. It should be noted that for both C_{Si} and Si_C antisites the number of s electrons is reduced by the lattice relaxation.

The values presented in table 1 show some deviations from those published in [8, 13] due to the improved method of calculations (the LDA + U approach) used in the present work.

3.2. Paired antisites

If two antisite defects are nearest neighbours of each other, the local tetrahedral symmetry around antisites is broken. In this case the defect atom is surrounded by three atoms of the same kind, the fourth neighbour being an atom of the other kind. Thus, we have to expect relaxation shifts which are different to those in the case of single antisite defects. The local symmetry around the antisite pair is decreased to C_{3v}, and the interatomic interaction tends to shift defect atoms along the $C_{Si}-Si_C$ axis. In fact, the C_{Si} antisite would be displaced closer to the three neighbouring C atoms, in order to shorten C–C bonds, whereas the Si_C antisite seems to be shifted towards its C_{Si} neighbour, in order to increase the Si–Si distance. Thus, for the antisite pair one expects the defect atoms to be shifted because of the lattice relaxation, while in the single-antisites case the nearest neighbours of the defects are displaced.

In our calculations we have used the following picture for the lattice relaxation. The changes in the interatomic distances were chosen to be 12% for the Si–Si_C bond and 8% for the C–C_{Si} bond, as in the case of single antisite defects. This choice requires only a small inwards shift of the carbon-atom neighbours of C_{Si}, the positions of the three silicon atoms bonded to Si_C being unchanged.

The calculated results for the antisite pair can be discussed in comparison with those obtained for single antisite defects. The total-energy considerations, even with the usual warnings as regards the errors that they could be affected by, because of the spherical approximation for the potential used in the ASA, show that the formation energy of the non-relaxed antisite pair is lower by 2.24 eV than the formation energy of two well-separated antisites. This value agrees well with results presented in [12], where the energy is reduced by 2.5 eV if two antisites combine to create the $C_{Si}-Si_C$ pair. However, it should be noted that, if the lattice relaxation is taken into account, this gain in the energy is substantially reduced and amounts only to 0.82 eV. This is the consequence of the lattice relaxation around the antisite pair leading to a small decrease of the total energy in comparison with that for the case of lattice relaxation around isolated antisites.

In the case of a non-relaxed antisite pair, the energy gap is equal to 1.54 eV and this value is very close to the one obtained for the single Si_C antisite. This means that the decreasing energy gap is caused also by the electron states related to the Si–Si bonds. The lattice relaxation leads to the value 1.03 eV, showing a stronger effect on the energy gap, due to the decreasing of the local symmetry and to the energy splitting of degenerate electron states at the band edges.

If we compare the valence DOS presented in figure 6 with those shown in figures 3 and

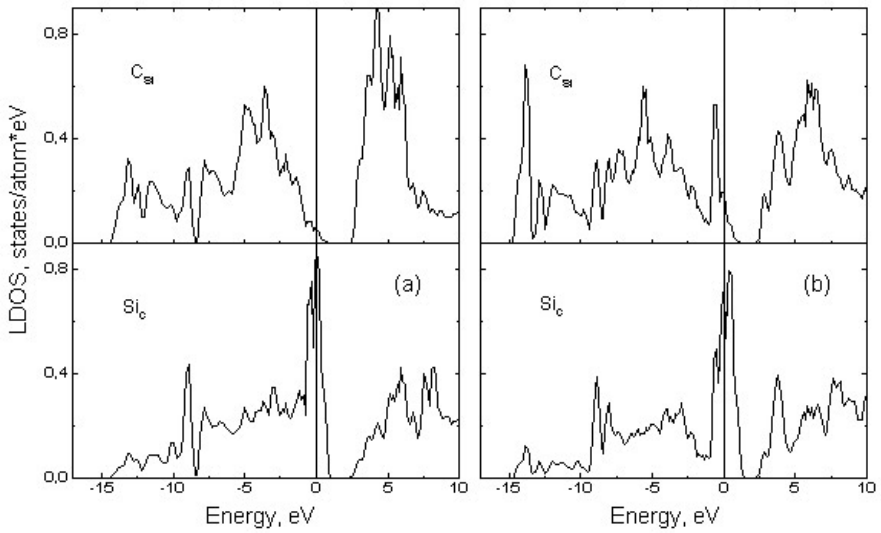

Figure 6. The calculated local densities of electron states for the antisite pair $C_{Si}-Si_C$ without (a) and with the lattice relaxation taken into account (b).

4, we can conclude that the main features of the case of single antisite defects are still present for paired antisites: there are resonance states at −8.72 eV (s) and just below the valence band top (p) for the Si_C antisite as well as resonance states at the bottom of the valence band (s) and at −5.51 eV (p) for the C_{Si} antisite. All peaks are shifted towards lower energies with respect to their positions obtained for single antisite defects. We should note also the splitting of p resonances caused by the decreasing of the local symmetry. The Si_C state at the top of the valence band is split into three peaks. The low-energy peak is related to the Si_C-C_{Si} bond and is reflected also in the local DOS of C_{Si} at −0.59 eV. Two other peaks should be ascribed mainly to Si–Si bonds. On the other hand, the Si_C local DOS in the conduction band is influenced by C_{Si} electron states giving rise to peaks in the energy range between +4 and +6 eV.

The valence electron charge localized in the atomic spheres (see figure 5) shows the same behaviour as for isolated antisite defects, even if the deviations from the values corresponding to *official* Si and C atoms are smaller. It should be noted that the lattice relaxation reduces these deviations considerably: the changes in the charge on the defect atoms are only about 0.2–0.3 electrons, which is comparable with charge perturbations at neighbouring atoms. The partial decomposition of the valence electron charge for paired antisites (shown in table 1) could be explained in much the same way as for single antisite atoms. Note the significant increasing of d components reflecting the reduced local symmetry around the Si_C-C_{Si} pair.

4. Optical properties

The changes in the energy band structure caused by point defects also affect the shape of the optical functions. The optical properties of silicon carbide are determined mainly by p → d transitions. The function $\varepsilon_1(\omega)$ shows its maximal values at about 6 eV and its minimal negative values at about 10 eV. The maximum of the function $\varepsilon_2(\omega)$ can be found at 7.5 eV. It can be seen in figure 7 that the presence of antisite defects modifies the fine structure of the dielectric

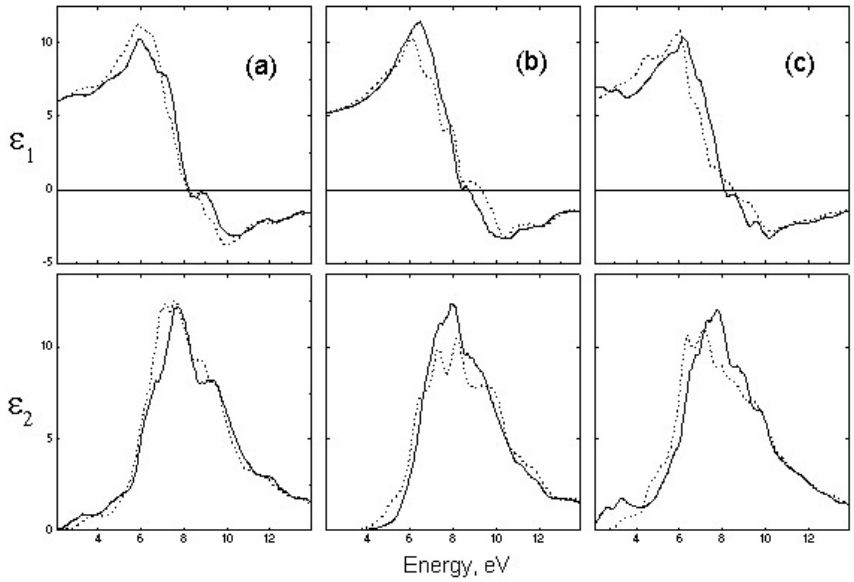

Figure 7. The real and imaginary parts of the dielectric function of β-SiC containing antisite defects: Si_C (a), C_{Si} (b) and the antisite pair $C_{Si}-Si_C$ (c) without (dashed curve) and with lattice relaxation (solid curve).

function, and these modifications are different for various kinds of defect. The changes in the shape of $\varepsilon(\omega)$ caused by lattice relaxation around point defects are comparable with differences between curves related to crystals with different kinds of defect. The prominent feature in the $\varepsilon_2(\omega)$ function, caused by Si_C antisites, is the low-energy structure at 3.3 eV, which reflects transitions from the p-like resonance state at the top of the valence band. This structure can be seen also in the case of paired antisites and it is absent for single C_{Si} defects. Another effect caused by presence of Si_C sites on the shape of dielectric function (especially $\varepsilon_2(\omega)$) is that the lattice relaxation leads to small energy shifts of peaks towards the high-energy side. This could be explained by the upwards shift of d states in the conduction band while the Si_C-Si distance increases. In the case of isolated C_{Si} antisites the lattice relaxation gives rise only to a variation of the peak intensities, and we can observe for the relaxed lattice an increasing intensity of most of the peaks in the dielectric function. For Si_C antisites as well as for paired antisites no significant increasing of intensity is obtained when the lattice relaxation is taken into account.

In figure 8 the real and imaginary parts of the dielectric function, as calculated both for the perfect β-SiC crystal and for the one containing the antisite defects, are shown and compared with the experimental data [30], taken for high-quality commercial crystals. No energy shift has been used in order to match theory and experiment. It can be seen that the computations for the perfect crystal reproduce very well the positions of the high-energy features: the minimum at 7.8 eV and the local maximum at 8.9 eV in $\varepsilon_1(\omega)$, as well as the minimum at 8.6 eV and the local maximum at 9.2 eV in $\varepsilon_2(\omega)$. In contrast, the low-energy part of the calculated dielectric function shows some deviations from the experimental results; for example, the main peak and the low-energy shoulder in $\varepsilon_2(\omega)$ are shifted upwards in energy. The calculated real part of the dielectric function $\varepsilon_1(\omega)$ is characterized by the prominent peak at 7.2 eV, just before the abrupt decreasing of the function. This narrow sharp peak occurs also in the calculations performed

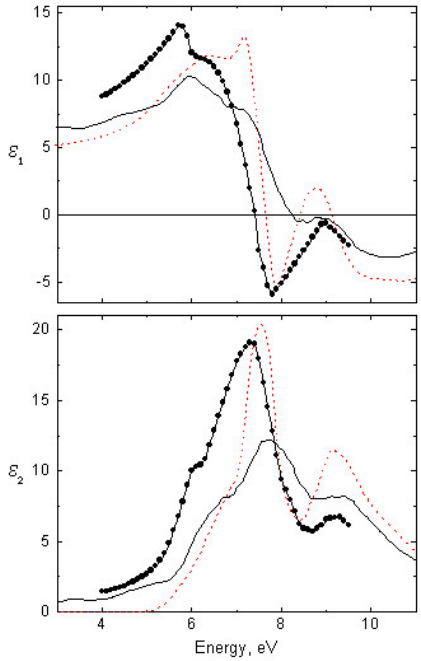

Figure 8. The real and imaginary parts of the dielectric function of β-SiC, as calculated for the perfect crystal (dashed curve), for the crystal containing Si_C antisite defects (solid curve) and measured experimentally [30] (solid circles).

by other methods (see, for example, [19]). In order to compare the calculated results with the experimental ones, the curves in figure 8 (as well as in figure 7) have been smoothed, but this peak remains the maximum of the function $\varepsilon_1(\omega)$. However, this peak is not observed in the experiment, and the maximal value is reached at the energy of 5.75 eV. It is obvious that this peak (close to the maximum of optical absorption) should be smeared more than other features if the lifetime of electron states is reduced due to scattering processes. In fact, this peak does not occur in the calculated dielectric functions for the crystals containing defects (see figure 7). The curves corresponding to crystals with single Si_C antisites have a shape which is closer to the experimental ones than those calculated with other kinds of defect. These curves are presented in figure 8 too. Apart from some energy shifts of the low-energy structures, the only disagreement with the experimental results is the reduced intensity of the calculated functions. This could be explained by the relatively high content of point defects in our model crystal calculations (almost 6% of sites are defects). On the other hand, it might be supposed that some minor defect concentrations in the specimens have affected the experimental data [30], and apparently these defects could be Si_C antisites.

5. Conclusions

In conclusion, by using an *ab initio* LMTO approach, we have computed the electronic structure of β-SiC containing antisite defects and the optical properties of both the perfect crystal and the crystal containing antisite defects. The LDA + U approach used in the present work gives rise to an improved description of both the electronic structure near the energy gap and the optical

functions. The attention has been mainly focused on the effects of the lattice relaxation around the defects on the electronic structure and optical properties of crystals. It has been shown that in β-SiC crystal the lattice relaxation leads usually to a decrease of the energy gap. For compositions deviating from the stoichiometric SiC, towards higher content of carbon atoms, the small reduction of the energy gap observed experimentally can be explained only if the lattice relaxation is taken into account and it is caused by the increased distance between the carbon atoms surrounding the C_{Si} antisite and the Si atoms (second neighbours of the defect).

The local electronic structure of antisite defects is characterized by s- and p-like resonance states in the valence band. Strong resonances occur also in the conduction band (especially for C_{Si}). The lattice relaxation modifies the energy distribution of unoccupied electron states, making it closer to that of the perfect crystal. The Si_C (C_{Si}) antisite has more (fewer) valence electrons localized in the atomic sphere than the *official* Si (C) atom, but this difference is considerably reduced by the lattice relaxation. It follows from the total-energy considerations that the creation of the antisite pair Si_C-C_{Si} is preferable to creation of isolated antisites, even if, when the lattice relaxation is taken into account, the energy gain is very small.

The presence of point defects modifies the shape of the optical functions as compared to the case for the perfect SiC crystal. For an accurate description of the optical properties of crystals containing point defects, it is necessary to take into account the lattice relaxation, due to its strong effect on the fine structure of the optical functions. Different kinds of defect lead to different shapes of optical functions. This offers an interesting possibility of distinguishing among different kinds of point defect by means of optical measurements. This problem requires however further theoretical as well as experimental investigations. The only way to test this hypothesis would be to increase the size of the supercell, in order to decrease the defect concentration, and to investigate the convergency of the calculated results towards the case of the perfect crystal. Unfortunately, this procedure is technically difficult because of the drastic increase in the computational effort required.

Acknowledgments

We are indebted to Professor G Foti and Professor G Mondio for stimulating discussions. This work was partially supported by NATO under Grant HTECH.CRG 970598.

References

[1] Lee K-H, Park C H, Cheong B-H and Chang K J 1994 *Solid State Commun.* **92** 869
[2] Park C H, Cheong B-H, Lee K-H and Chang K J 1994 *Phys. Rev.* B **49** 4485
[3] Lambrecht W R L, Segall B, Yoganathan M, Suttrop W, Devaty R P, Choyke W J, Edmond J A, Powell J A and Alouani M 1994 *Phys. Rev.* B **50** 10 722
[4] Käckel P, Wenzien B and Bechstedt F 1994 *Phys. Rev.* B **50** 10 761
[5] Käckel P, Wenzien B and Bechstedt F 1994 *Phys. Rev.* B **50** 17 037
[6] Wenzien B, Käckel P, Bechstedt F and Capellini G 1995 *Phys. Rev.* B **52** 10 897
[7] Persson C and Lindefelt U 1996 *Phys. Rev.* B **54** 10 257
[8] Cubiotti G, Kucherenko Yu and Antonov V N 1997 *J. Phys.: Condens. Matter* **9** 165
[9] Li Y and Lin-Chung P J 1987 *Phys. Rev.* B **36** 1130
[10] Talwar D N and Feng Z C 1991 *Phys. Rev.* B **44** 3191
[11] Liu Wenchang, Zhang Kaiming and Xie Xide 1993 *J. Phys.: Condens. Matter* **5** 891
[12] Wang C, Bernholc J and Davis R F 1988 *Phys. Rev.* B **38** 12 752
[13] Cubiotti G, Kucherenko Yu, Yaresko A, Perlov A and Antonov V N 1998 *J. Electron Spectrosc. Relat. Phenom.* 1998 **88–91** 957
[14] Andersen O K 1975 *Phys. Rev.* B **12** 3060
[15] Skriver H L 1984 *The LMTO Method* (Berlin: Springer)

[16] von Barth U and Hedin L 1971 *J. Phys. C: Solid State Phys.* **4** 2064
[17] Blöchl P E, Jepsen O and Andersen O K 1994 *Phys. Rev.* B **49** 16 223
[18] Ehrenreich H and Cohen M A 1959 *Phys. Rev.* **115** 786
[19] Adolph B, Gavrilenko V I, Tenelsen K, Bechstedt F and Del Sole R 1996 *Phys. Rev.* B **53** 9797
[20] Anisimov V I, Aryasetiawan F and Lichtenstein A I 1997 *J. Phys.: Condens. Matter* **9** 767
[21] Anisimov V I, Zaanen J and Andersen O K 1991 *Phys. Rev.* B **44** 943
[22] Anisimov V I, Solovyev I V, Korotin M A, Czyzyk M T and Sawatzky G A 1993 *Phys. Rev.* B **48** 16 929
[23] Hedin L 1965 *Phys. Rev.* **139** A796
[24] Hedin L and Lundqvist S 1969 *Solid State Physics* vol 23, ed H Ehrenreich, F Seitz and D Turnbull (New-York: Academic) p 1
[25] Bechstedt F, Fiedler M, Kress C and Del Sole R 1994 *Phys. Rev.* B **49** 7357
[26] *Landolt–Börnstein New Series* 1982 Group III, vol 17a, ed O Madelung (Berlin: Springer)
[27] Humphreys R G, Bimberg D and Choyke W J 1981 *Solid State Commun.* **39** 163
[28] Philipp H R and Taft E A 1964 *Phys. Rev.* **136** A1445
[29] Philipp H R and Ehrenreich H 1963 *Phys. Rev.* **129** 1550
[30] Logothetidis S and Petalas J 1996 *J. Appl. Phys.* **80** 1768
[31] Torpo L, Pöykkö S and Nieminen R M 1998 *Phys. Rev.* B **57** 6243
[32] Robertson J 1992 *Phil. Mag.* B **66** 615
[33] Sussman R S and Ogden R 1981 *Phil. Mag.* B **44** 137
[34] Mui K, Basa D K, Smith F W and Corderman R 1987 *Phys. Rev.* B **35** 8089
[35] Kuhman D, Grammatica S and Jansen F 1989 *Thin Solid Films* **177** 253